

Dyes produced by the reaction of 1,2,3,4-tetrafluoro-9,10-anthraquinones with bifunctional nucleophiles

Masaki Matsui^{a,*}, Shinobu Taniguchi^a, Masayuki Suzuki^a, Mingxing Wang^a,
Kazumasa Funabiki^a, Hisayoshi Shiozaki^b

^aDepartment of Materials Science and Technology, Faculty of Engineering, Gifu University, 1-1 Yanagido, Gifu 501-1193, Japan

^bTechnology Research Institute of Osaka Prefecture, 2-7-1 Ayumino, Izumi, Osaka 594-1157, Japan

Received 7 May 2004; received in revised form 10 July 2004; accepted 14 July 2004

Available online 29 September 2004

Abstract

1,2,3,4-Tetrafluoro-9,10-anthraquinones reacted with a molar amount of bifunctional nucleophiles, such as 2-aminophenol, catechol, 2-aminobenzenethiol, ethylenediamine, and 1,4-butanediamine to produce the 1,2-cyclized products, which further reacted with another molar amount of bifunctional nucleophiles to afford the dicyclized derivatives.

© 2004 Elsevier Ltd. All rights reserved.

Keywords: Anthraquinone dyes; Bifunctional nucleophiles; Fluorine; Photostability

1. Introduction

9,10-Anthraquinone derivatives are important compounds due to their applications in dyes and pigments [1]. Since fluorine-containing dyes show unique properties, they have potential applications to advanced materials [2]. Meanwhile, fluorine atoms in the aromatic moiety can act as leaving groups under nucleophilic substitution reaction conditions. 1-Fluoro-9,10-anthraquinone reacts with *N,N*-dimethylhydrazine to give the dimethylamino-substituted and pyrazole derivatives depending on the solvent and reaction temperature [3]. 1-Fluoro- and 1,4-difluoro-9,10-anthraquinone derivatives react with 2-[(2-aminoethyl)amino]ethanol to provide the substitution products [4,5]. 1,4-Difluoro-9,10-anthraquinones undergo *ipso*-substitutions by amines or

diamines to provide the 1,4-disubstituted derivatives [6]. The reaction of 1,2,3,4-tetrafluoro-9,10-anthraquinone with nucleophiles such as amines [7–9] and methoxide ion [10,11] has been reported to give both the 1- and 2-substituted derivatives depending on the kinds of nucleophiles, solvents, and reaction temperature. Arenethiols have been reported to react with 1,2,3,4-tetrafluoro-9,10-anthraquinone to provide the 2,3-bis(arylthio) derivatives [12]. These products have potential applications as toners, inks for dye diffusion thermal transfer printing, and color filters [13]. The reaction of 2,3-dibromo-5,6,7,8-tetrafluoro-1,4-dihydroxy-9,10-anthraquinone with potassium 2-aminobenzenethiolate or zinc 2-aminobenzeneselenate to give 11*H*,18*H*-13,14,15,16-tetrafluoro-11,18-diaza-5,6-dithia- and -diselenatrinaphthylene-12,17-diones has been reported, the fluoroaromatic moiety being unchanged [14–16]. Though 11*H*,18*H*-11,18-diaza-5,6-dithia- and -diselenatrinaphthylene-12,17-diones have also been synthesized by this reaction [17], no other dicyclized derivatives have been synthesized so far. Thus, fluorine-containing anthraquinones are interesting compounds from

* Corresponding author. Tel.: +81 58 293 2601; fax: +81 58 230 1893.

E-mail address: matsui@apchem.gifu-u.ac.jp (M. Matsui).

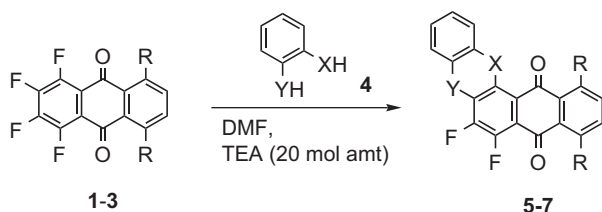
the viewpoint of both their reactions and applications. When 1,2,3,4-tetrafluoro-9,10-anthraquinone reacts with bifunctional nucleophiles, novel anthraquinone derivatives are obtained. We report herein the dyes derived from the reaction of 1,2,3,4-tetrafluoro-9,10-anthraquinones with bifunctional nucleophiles.

2. Results and discussion

The reaction of 1,2,3,4-tetrafluoro-9,10-anthraquinones **1–3** with aromatic bifunctional nucleophiles **4a–c** is shown in Scheme 1 and Table 1. The reaction of 1,2,3,4-tetrafluoro-9,10-anthraquinone (**1**) with **4a** at 30 °C in the absence of triethylamine (TEA) was slow and afforded the 1,2-cyclized derivative **5a** in an 11% yield (entry 1). However, the reaction in the presence of 10 and 20 molar amounts of TEA was fast and preferentially gave **5a** in 35 and 81% yields, respectively (entries 2 and 3). Thus, compound **1** smoothly reacted with **4a** to give **5a** under mild conditions in the presence of TEA. The reactivity of 2-aminobenzenethiol (**4c**) with **1** was higher than those of **4a** and catechol (**4b**) with **1** (entries 3–5). The reaction of **4c** with **1** formed unidentified products which were not developed by column chromatography. Compounds **2** and **3** also reacted with **4** to give the 1,2-cyclized products **6** and **7**, respectively (entries 6–9). The reaction of **1** with *o*-phenylenediamine was very complicated and gave several unidentified products.

The products **5a** and **5c** showed their NH-proton peaks come from the intramolecular hydrogen bonding with quinonoid-oxygen atoms at 11.07 and 12.19 ppm in the ¹H NMR spectroscopy, respectively. The ¹⁹F NMR spectra of **5a**, **5b**, and **5c** showed a pair of typical doublet *o*-fluorine atoms *J* = 18.9, 20.6, and 20.4 Hz, respectively.

The reaction of **1** with ethylenediamine (**4d**) and 1,4-butanediamine (**4e**) is shown in Scheme 2. Only 1,2-cyclized products **5d** and **5e** were isolated in these reactions. The reaction of **1** with 1,6-hexanediamine was complicated and gave many unidentified products. Both **5d** and **5e** showed proton peaks based on intramolecular hydrogen bonding at 9.97 and 10.27 ppm, respectively. A set of *o*-fluorine peaks was observed for **5d** (*J* = 19.1 Hz) and **5e** (*J* = 21.7 Hz).



Scheme 1.

1,2-Cyclized products **5** and **7** reacted with another molar amount of bifunctional nucleophiles **4** to afford the dicyclized 9,10-anthraquinone derivatives **8–15** as shown in Scheme 3 and Table 2. Compared with the reaction of **1** with **4** to give the 1,2-cyclized products **5** as shown in Table 2, more severe reaction conditions were required to form **8–15**. In the reaction of **4c** with **5c**, unidentified products which were not developed by column chromatography were produced. Thus, not only symmetrical derivatives **8**, **12**, **14**, and **15** but also unsymmetrical ones **9**, **10**, **11**, and **13** were obtained by this stepwise reaction.

It is known that the introduction of electron-donating amino groups at the 1-, 4-, 5-, and 8-positions in an anthraquinone skeleton causes a bathochromic shift. The absorption maxima (λ_{\max}) of 1-amino-1,4-diamino-, and 1,4,5,8-tetraamino-9,10-anthraquinones were observed at 464, 582, and 619 nm in dichloromethane, respectively. To obtain a near-infrared absorbing dye, the dichloro derivative **15** was reacted with *p*-anisidine (**16**) in the presence of sodium acetate to give the di(4-anisidino) derivative **17** in a 39% yield as shown in Scheme 4.

The UV–vis absorption spectra of **5c**, the corresponding fluorine-free 14*H*-naphtho[2,3-*a*]phenothiazine-8,13-dione (**5'c**), **14**, and **17** are shown in Fig. 1. The compounds **5c** and **5'c** showed the first absorption band at 579 and 588 nm, respectively, there being no remarkable difference. Compound **14** showed the first absorption band at 689 nm. As expected, compound **17** was even more bathochromic, showing the λ_{\max} at 800 nm.

The UV–vis absorption spectra of the other anthraquinone derivatives are indicated in Table 3. 1,2-Cyclized derivatives **5** were more bathochromic in the following order: **5c** (579 nm) > **5a** (550) > **5b** (353). Dicyclized derivatives **8–15** were more bathochromic than the 1,2-cyclized derivatives **5–7**. For example, the λ_{\max} of **14** and **5c** were observed at 689 and 579 nm, respectively. Symmetrically dicyclized derivatives were more bathochromic in the following order: **14** (*X*=*X'*=NH, *Y*=*Y'*=S, 689) > **8** (*X*=*X'*=NH, *Y*=*Y'*=O, 642) \gg **12** (*X*=*X'*=*Y*=*Y'*=O, 414). The λ_{\max} of unsymmetrically dicyclized derivatives was observed between those of the corresponding symmetrical ones. For example, the λ_{\max} of **10** (*X*=*X'*=NH, *Y*=O, *Y'*=S, 664) was observed between those of **8** (642) and **14** (689).

After geometry optimization of the compounds by the B3LYP/3-21G method with Gaussian 03W program [18], the absorption spectra were studied with the INDO/S method implemented in WinMOPAC program to analyze the chromophoric system. In the INDO/S calculation, the parameters of fluorine and sulfur atoms (F: E_s = 43.70, E_p = 20.89, B_{sp} = 50.0, G = 17.36; S: E_s = 21.02, E_p = 10.97, B_{sp} = 13.5, G = 10.01) were

Table 1
Reaction of 1,2,3,4-tetrafluoro-9,10-anthraquinones **1–3** with bifunctional nucleophiles **4**^a

Entry	Starting material		Bifunctional nucleophile			Reaction conditions		Product				
	Compound	R	Compound	X	Y	Temp./°C	Time/h	Compound	R	X	Y	Yield ^b /%
1 ^c	1	H	4a	NH	O	30	6	5a	H	NH	O	11 ^d
2 ^e	1	H	4a	NH	O	30	6	5a	H	NH	O	35
3	1	H	4a	NH	O	30	4	5a	H	NH	O	81
4	1	H	4b	O	O	30	6	5b	H	O	O	84
5	1	H	4c	NH	S	0	4	5c	H	NH	S	21
6	2	OH	4a	NH	O	30	4	6a	OH	NH	O	48
7	2	OH	4b	O	O	30	6	6b	OH	O	O	29 ^f
8	2	OH	4c	NH	S	0	3	6c	OH	NH	S	13 ^g
9	3	Cl	4c	NH	S	0	2	7c	Cl	NH	S	51 ^h

^a All reactions were carried out with 0.5 mmol of substrate and bifunctional nucleophiles (0.55 mmol) in the presence of TEA (10 mmol) in DMF (15 mL) otherwise cited. The conversion of starting material was 100% otherwise cited.

^b Isolated yields.

^c In the absence of TEA.

^d Thirty-five percent conversion.

^e In the presence of 10 molar amounts of TEA (5 mmol).

^f 6,13-Difluoro-8,11-dihydroxynaphtho[2,3-*b*]oxanthrene-7,12-dione (**6b'**) was also isolated in a 59% yield.

^g Eighty-five percent conversion.

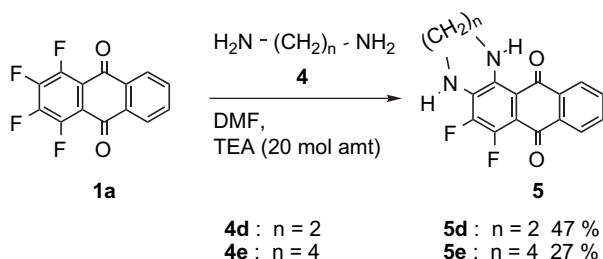
^h 11*H*, 18*H*-13,16-Dichloro-11,18-diaza-5,6-dithiatrinaphthylene-12,17-dione (**15**) was also obtained in a 20% yield.

added [19]. Four hundred configurations were considered for the configuration interaction. The results are also shown in Table 3. The first absorption bands of 1,2-cyclized derivatives **5–7** were attributed to the HOMO to LUMO transition. The figures of HOMO, LUMO, and the difference in electron density accompanied by the first excitation of **5c** are shown in Fig. 2. The figure in the HOMO energy level suggests that the electronic effect at the hetaryl moieties plays an important role for the absorption band. The first absorption band of **5c** was attributed to an intramolecular charge-transfer chromophoric system from the phenothiazino to naphthoquinone moiety.

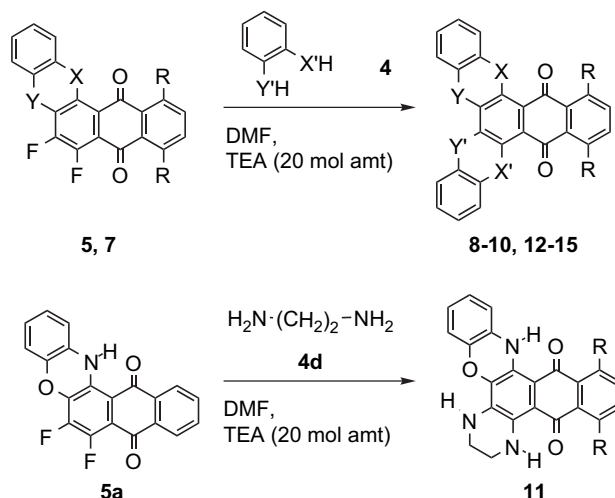
The HOMO and LUMO energy levels of **5** are shown in Fig. 3. No remarkable difference in the LUMO energy level was calculated for **5a**, **5b**, and **5c** (−1.8367 to −1.7362 eV). Meanwhile, the energy level of HOMO showed significant difference and was lower in the following order: **5b** (−8.4377) > **5a** (−7.6449) > **5c** (−7.5929). Therefore, the bathochromicity of 1,2-cyclized derivatives **5** could be attributed to higher HOMO energy level by introducing the electron-donating hetero atoms such as nitrogen into the

molecule. No remarkable differences in the HOMO and LUMO energy levels between **5c** and **5'c** were calculated, suggesting similar UV–vis absorption spectra.

The typical UV–vis absorption band of **14** is depicted in Fig. 1. Compound **14** showed first absorption band at 689 nm. The UV–vis absorption spectral data of the other dicyclized derivatives **8–13** and **15** are also indicated in Table 3. The first absorption bands of **14** were also attributed to the HOMO to LUMO transition. The figures of HOMO, LUMO, and difference in electron density accompanied by the first excitation of **14** are shown in Fig. 4. The compound **14** was also analyzed as an intramolecular charge-transfer chromophoric system from the hetaryl to naphthoquinone moiety. The first absorption bands of dicyclized derivatives **8–15** were more bathochromic than the



Scheme 2.



Scheme 3.

Table 2
Reaction of 1,2-difluoro-9,10-anthraquinones **5** and **7** with bifunctional nucleophiles **4**^a

Entry	Starting material				Bifunctional nucleophile			Reaction conditions		Product						
	Compound	R	X	Y	Compound	X'	Y'	Temp./°C	Time/h	Compound	R	X	Y	X'	Y'	Yield ^b /%
1	5a	H	NH	O	4a	NH	O	90	24	8	H	NH	O	NH	O	35
2	5a	H	NH	O	4b	O	O	120	24	9	H	NH	O	O	O	62
3	5a	H	NH	O	4c	NH	S	30	24	10	H	NH	O	NH	S	55
4	5a	H	NH	O	4d	—	—	60	36	11	—	—	—	—	—	31
5	5b	H	O	O	4b	O	O	120	9	12	H	O	O	O	O	94
6	5b	H	O	O	4c	NH	S	0	24	13	H	O	O	NH	S	40
7	5c	H	NH	S	4c	NH	S	30	6	14	H	NH	S	NH	S	26
8	7c	Cl	NH	S	4c	NH	S	0	2	15	Cl	NH	S	NH	S	78

^a All reactions were carried out with 0.5 mmol of substrate and bifunctional nucleophiles (0.55 mmol) in the presence of TEA (10 mmol) in DMF (15 mL) otherwise cited. The conversion of starting material was 100% otherwise cited.

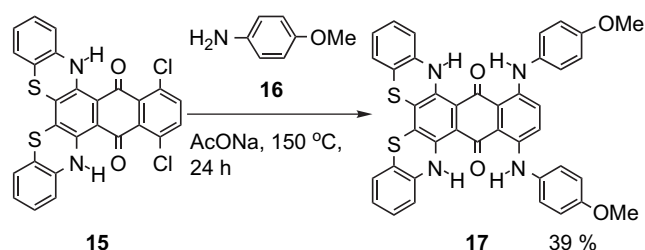
^b Isolated yields.

corresponding 1,2-cyclized derivatives **5**–**7**. The HOMO and LUMO energy levels of **14** are shown in Fig. 3. The LUMO energy levels of **14** and **5c** were calculated to be -1.7215 and -1.8288 eV, respectively, there being no remarkable difference. Meanwhile, the HOMO energy level of **14** (-6.9541 eV) was much higher than that of **5c** (-7.5929). Thus, the bathochromicity of dicyclized derivatives **8**–**15**, compared with the corresponding 1,2-cyclized derivatives **5**–**7**, is mainly attributed to the higher HOMO energy level. The first absorption band of symmetrically dicyclized derivatives was more bathochromic in the following order: **14** (689 nm) > **8** (642) >> **12** (414). Though no remarkable difference in the LUMO energy levels (-1.5893 to -1.7215 eV) was calculated among them, significant difference was calculated for their HOMO energy levels (-8.0966 to -6.9541). Thus, the bathochromicity of dicyclized derivatives **8**–**15** could be attributed to the higher HOMO energy level by introducing electron-donating hetero atoms into the molecule.

It is of interest to compare the melting point of fluorine-containing derivatives with that of fluorine-free ones because fluorine-containing derivatives can show lower melting point due to less intermolecular interactions. The example is shown in Fig. 5. The melting point of fluorine-containing derivative **5c** (202 °C) was lower than the corresponding fluorine-free derivative **5'c** (274–275) [20]. Meanwhile, the melting points of **5d** (268–270) and 1-diethylamino-2,3,4-trifluoro-9,10-

anthraquinone (**5f**, 144–146) [21] were higher than those of naphtho[2,3-*f*]-1,2,3,4-tetrahydroquinoxalin-7,12-dione (**5'd**, 190.0–191.0) [22] and 1-diethylamino-9,10-anthraquinone (**5'f**, 83–84), respectively. Thus, the melting points of fluorine-containing anthraquinone derivatives were not always lower than that of fluorine-free ones.

The photostability of **5c**, **5'c**, and **14** is shown in Fig. 6. The stability was in the following order of dyes: **14** > **5'c** > **5c**. The reduction (E_{red}) and oxidation potentials (E_{ox}) of these compounds are shown in Table 4. The order of photostability was consistent with that of E_{red} and not with that of E_{ox} . Since fluorine atom has electron-withdrawing nature, it is reasonable that the E_{red} of **14** was most negative among **5c**, **5'c**, and **14**. This result suggests that compound **14** is most stable against the reduction processes. The photodecomposition of anthraquinone dyes in solution has been reported to proceed by way of reduction processes [23,24]. It is concluded that the introduction of fluorine atom(s) into 9,10-anthraquinone dyes does not improve the photostability.



Scheme 4.

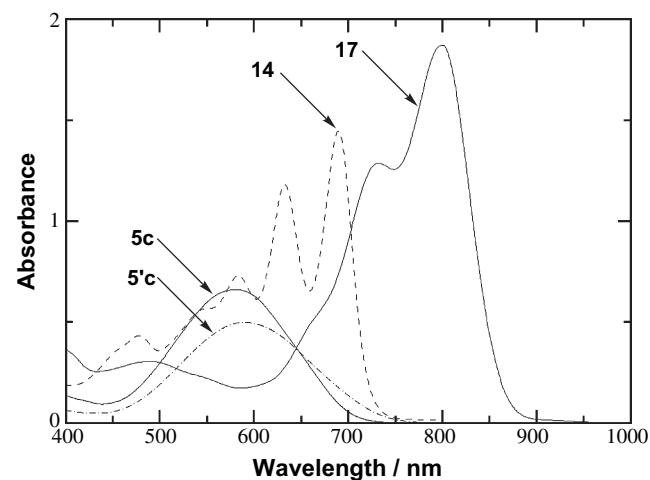


Fig. 1. UV-vis absorption spectra of **5c**, **5'c**, **14**, and **17**. Measured in dichloromethane at a concentration of $0.66 \text{ mmol dm}^{-3}$.

Table 3
Observed and calculated UV–vis absorption bands of anthraquinone dyes

Compound	Observed ^a	Calculated	
	λ_{\max} (ϵ)/nm	λ_{\max} (f^b)	Assignment (canonical orbital energy, eV) (CI coefficient)
1	329 (5800)	— ^c	— ^c
2	499 (8400)	— ^c	— ^c
3	355 (4500)	— ^c	— ^c
5a	550 (8400)	453 (0.3544)	HOMO (−7.6449)–LUMO (−1.8367) (86%)
5b	353 (5700)	351 (0.2189)	HOMO (−8.4377)–LUMO (−1.7362) (64%)
5c	579 (9100)	458 (0.3493)	HOMO (−7.5929)–LUMO (−1.8288) (86%)
5'c	588 (7500)	456 (0.3519)	HOMO (−7.3776)–LUMO (−1.6338) (86%)
5d	516 (11 300)	426 (0.3333)	HOMO (−7.7319)–LUMO (−1.6182) (82%)
5e	535 (9800)	418 (0.2951)	HOMO (−7.8502)–LUMO (−1.6645) (73%)
6a	591 (10 900)	490 (0.5590)	HOMO (−7.7389)–LUMO (−2.2229) (86%)
6b	490 (7600)	423 (0.4793)	HOMO (−8.3302)–LUMO (−2.1483) (90%)
6b'	497 (9200)	419 (0.4414)	HOMO (−8.3555)–LUMO (−2.1235) (94%)
6c	619 (9800)	496 (0.5469)	HOMO (−7.6845)–LUMO (−2.2143) (86%)
7c	354 (5100), 582 (8100)	470 (0.3519)	HOMO (−7.6819)–LUMO (−2.0523) (86%)
8	592 (16 000), 642 (19 000)	388 (0.3442)	NHOMO (−7.7227)–LUMO (−1.6688) (63%), HOMO (−7.0598)–NLUMO (−0.2612) (27%)
9	389 (5200), 567 (9100)	518 (0.4813) 334 (0.2476)	HOMO (−7.0598)–LUMO (−1.6688) (93%) NHOMO (−8.1766)–LUMO (−1.5893) (39%), HOMO (−7.3565)–NLUMO (−0.2430) (38%)
10	611 (9200), 664 (7800)	460 (0.3666) 388 (0.3445)	HOMO (−7.3565)–LUMO (−1.5893) (87%) NHOMO (−7.7403)–LUMO (−1.6798) (53%), HOMO (−7.0139)–NLUMO (0.2374) (33%)
11	574 (17 000), 620 (19 000)	526 (0.4803) 429 (0.8873)	HOMO (−7.0139)–LUMO (−1.6798) (93%) NHOMO (−7.5439)–LUMO (−2.3879) (10%), HOMO (−5.9194)–NLUMO (0.3158) (10%)
12	414 (4500)	554 (0.3399) 370 (0.2196)	NHOMO (−7.5439)–LUMO (−2.3879) (79%) HOMO (−8.0966)–LUMO (−1.5893) (87%)
13	414 (6600), 592 (11 000)	330 (0.3145) 467 (0.3672) 393 (0.3547)	NHOMO (−8.1939)–LUMO (−1.5936) (33%), HOMO (−7.3121)–NLUMO (−0.2125) (45%) HOMO (−7.3121)–LUMO (−1.5936) (87%) NHOMO (−7.7440)–LUMO (−1.7215) (50%), HOMO (−6.9541)–NLUMO (−0.2329) (33%)
14	633 (17 000), 689 (21 000)	543 (0.4768) 402 (0.3460)	HOMO (−6.9541)–LUMO (−1.7215) (94%) NHOMO (−7.8227)–LUMO (−1.9373) (60%), HOMO (−7.0444)–NLUMO (−0.5463) (24%)
15	656 (3900), 712 (3500)	561 (0.4959) 635 (0.8377)	HOMO (−7.0444)–LUMO (−1.9373) (94%) HOMO (−6.5343)–LUMO (−1.7801) (93%)
17	733 (19 000), 800 (28 000)		

^a Measured in dichloromethane.

^b Oscillator strength.

^c Not calculated.

3. Experimental

3.1. Instruments

Melting points were measured with a Yanagimoto MP-S2 micro-melting-point apparatus. NMR spectra were recorded on Varian Inova 400 and 500 spectrometers. Mass spectra were taken on a Shimadzu QP-1000 spectrometer. Elemental analysis was performed with a Yanaco MT-6 CHN coder. UV–vis absorption spectra were measured with Shimadzu UV-160A and Hitachi U-3500 spectrometers. Cyclic voltammetry was measured with a CHI (CH instrument, Austin, Texas) model 660 electrochemical analyzer. Thermogravimetric

differential thermal analysis (TG-DTA) was performed by a Rigaku TAS-200 instrument.

3.2. Materials

2-Aminophenol (**4a**), catechol (**4b**), 2-aminobenzene-thiol (**4c**), ethylenediamine (**4d**), 1,4-butanediamine (**4e**), and *p*-anisidine (**16**) were purchased from Tokyo Kasei Co., Ltd. 1,2,3,4-Tetrafluoro-5,8-dihydroxy-9,10-anthraquinone (**2**) was obtained from Sigma–Aldrich Co., Ltd. 1,2,3,4-Tetrafluoro-9,10-anthraquinone (**1**) [10], 5,8-dichloro-1,2,3,4-tetrafluoro-9,10-anthraquinone (**3**) [10], and 14*H*-naphtho[2,3-*a*]phenothiazine-8,13-dione (**5'c**) [20] were prepared as described in the

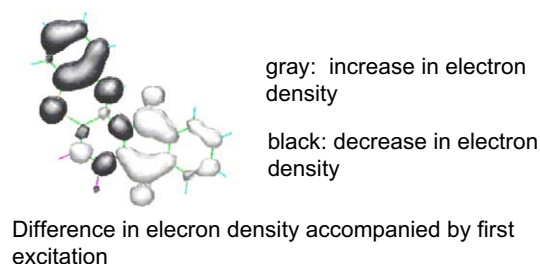
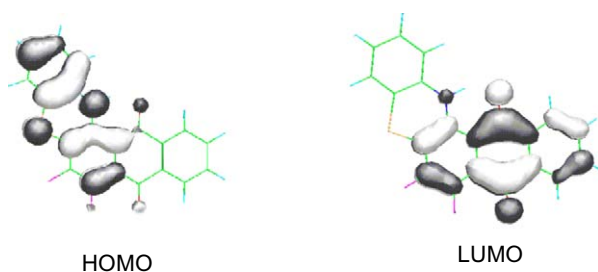


Fig. 2. HOMO, LUMO, and difference in electron density accompanied by first excitation of **5c**.

literature. 1-Diethylamino-9,10-anthraquinone was synthesized as described in literature [25] and its melting point was measured to be 83–84 °C.

3.3. Reaction of fluorine-containing 9,10-anthraquinones **1–3**, **5**, and **7** with bifunctional nucleophiles **4**

To a DMF solution (15 mL) of fluorine-containing 9,10-anthraquinones **1–3**, **5**, and **7** (0.5 mmol) were added bifunctional nucleophiles **4** (0.55 mmol) and triethylamine (TEA, 10 mmol). After the reaction was completed, the mixture was poured into brine (100 mL). The resulting precipitate was filtered, purified by silica-gel column chromatography (**5a**, **5b**, **5c**, **6a**, **6b**, **6b'**, **6c**,

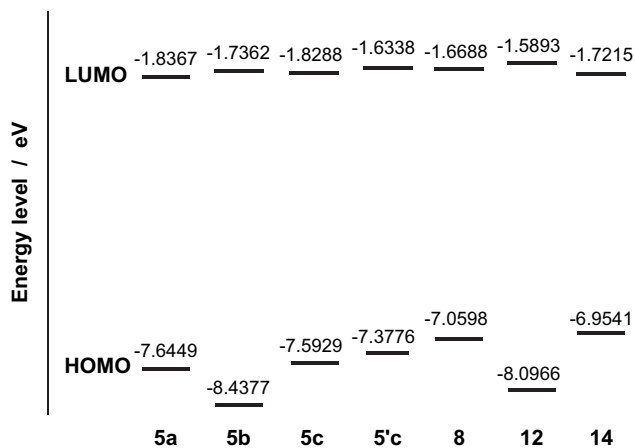


Fig. 3. HOMO and LUMO energy levels of selected anthraquinone derivatives.

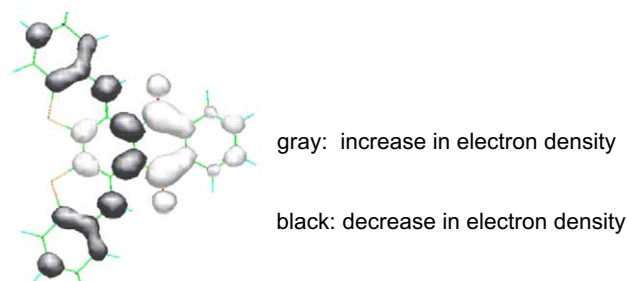
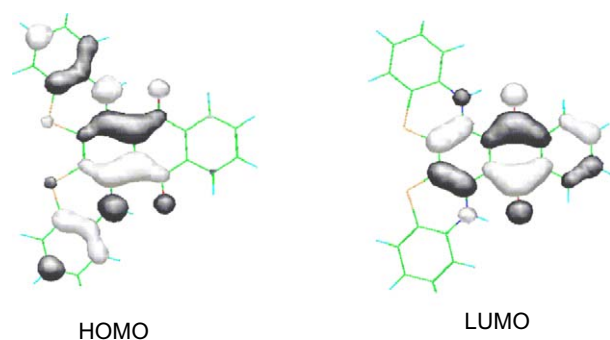


Fig. 4. HOMO, LUMO, and difference in electron density accompanied by first excitation of **14**.

Fig. 4. HOMO, LUMO, and difference in electron density accompanied by first excitation of **14**.

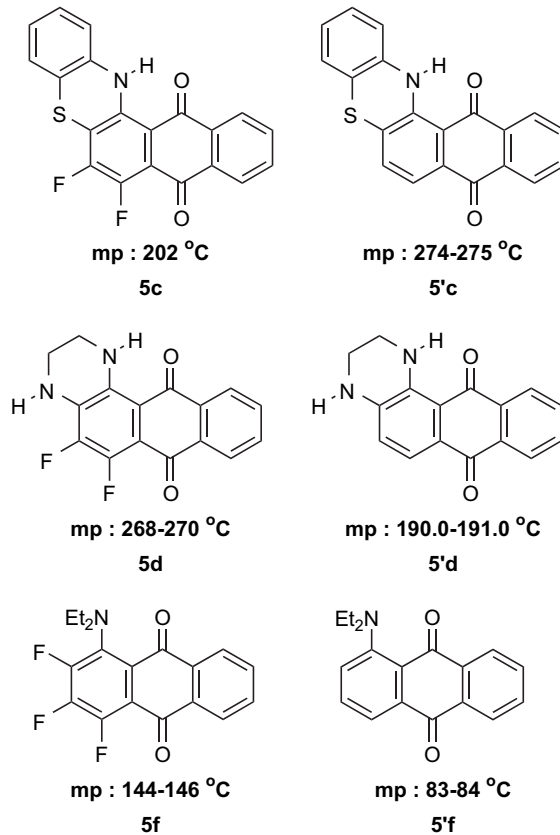


Fig. 5. Comparison of melting points between fluorine-containing and fluorine-free anthraquinone derivatives.

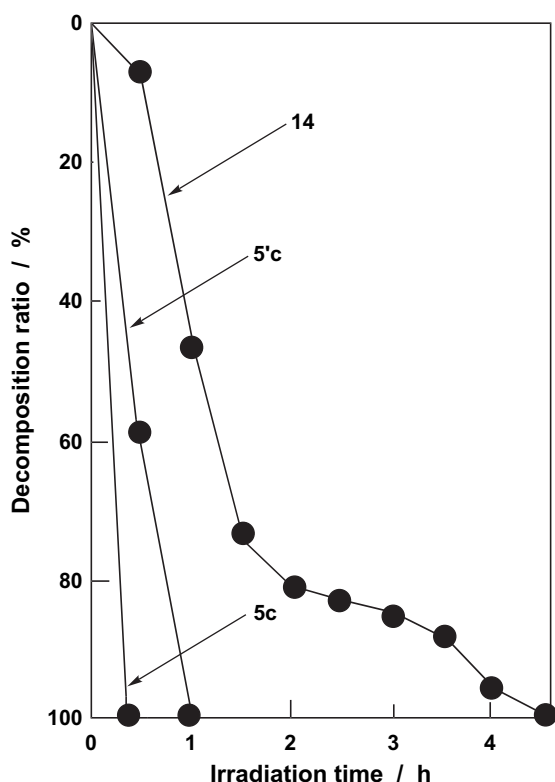


Fig. 6. Photostability of **5c**, **5'c**, and **14**. A dichloromethane solution (13 mL) of substrate (1.08×10^{-2} mmol dm $^{-3}$) was irradiated with a 300-W high-pressure mercury lamp by using a merry-go-round at 25 °C under an air atmosphere. The UV–vis absorption spectra were measured. The decomposition ratio (%) was calculated on the basis of the absorbance at the absorption maxima.

7c, **9**, **10**, **13**, **14**, **15**: toluene; **8**, **12**: toluene/hexane = 1/1; **5d**, **5e**, **11**: dichloromethane), and recrystallized (**5a**, **5b**, **5c**, **5d**, **5e**, **6b**, **6b'**, **7c**, **11**, **15**: toluene; **6a**, **6c**, **8**, **9**, **10**, **12**, **13**, **14**: chloroform–hexane). The physical and spectral data of products are given below.

3.3.1. 6,7-Difluoro-14H-naphtho[2,3-a]phenoxazine-8,13-dione (**5a**)

Mp 263 °C; ^1H NMR (400 MHz, CDCl_3) δ = 6.66 (d, J = 7.3 Hz, 1H), 6.82–6.84 (m, 2H), 6.90–6.94 (m, 1H), 7.78–7.80 (dd, J = 2.8 and 1.3 Hz, 2H), 8.25 (dd,

J = 2.8 and 1.3 Hz, 2H), 11.07 (s, 1H); ^{19}F NMR (376 MHz, CDCl_3 , ext. CF_3COOH) δ = –70.47 (d, J = 18.9 Hz, 1F), –62.62 (d, J = 18.9 Hz, 1F); EIMS m/z (%) 349 (M^+ ; 100), 264 (24), 245 (24), 216 (34). Anal. Calcd for $\text{C}_{20}\text{H}_9\text{F}_2\text{NO}_3$: C, 68.77; H, 2.60; N, 4.01%. Found: C, 68.68; H, 2.75; N, 3.99%.

3.3.2. 6,7-Difluoronaphtho[2,3-a]oxanthrene-8,13-dione (**5b**)

Mp 220 °C; ^1H NMR (400 MHz, CDCl_3) δ = 7.05–7.06 (m, 4H), 7.80 (dd, J = 5.9 and 3.3 Hz, 2H), 8.24 (dd, J = 5.9 and 3.3 Hz, 2H); ^{19}F NMR (376 MHz, CDCl_3 , ext. CF_3COOH) δ = –70.49 (d, J = 20.6 Hz, 1F), –63.83 (d, J = 20.6 Hz, 1F); EIMS m/z (%) 350 (M^+ ; 100), 322 (8), 294 (14). Anal. Calcd for $\text{C}_{20}\text{H}_8\text{F}_2\text{O}_4$: C, 68.58; H, 2.30%. Found: C, 68.52; H, 2.78%.

3.3.3. 6,7-Difluoro-14H-naphtho[2,3-a]-phenothiazine-8,13-dione (**5c**)

Mp 202 °C; ^1H NMR (400 MHz, CDCl_3) δ = 6.73 (d, J = 7.3 Hz, 1H), 6.89–6.90 (m, 2H), 7.04–7.08 (m, 1H), 7.76–7.83 (m, 2H), 8.24–8.29 (m, 2H), 12.19 (s, 1H); ^{19}F NMR (376 MHz, CDCl_3 , ext. CF_3COOH) δ = –66.75 (d, J = 20.4 Hz, 1F), –45.97 (d, J = 20.4 Hz, 1F); EIMS m/z (%) 365 (M^+ ; 100), 309 (15), 277 (10). Anal. Calcd for $\text{C}_{20}\text{H}_9\text{F}_2\text{NO}_2\text{S}$: C, 65.75; H, 2.48; N, 3.83%. Found: C, 65.93; H, 2.76; N, 3.83%.

3.3.4. 5,6-Difluoro-1,2,3,4-tetrahydronaphtho-[2,3-f]quinoxaline-7,12-dione (**5d**)

Mp 268–270 °C; ^1H NMR (400 MHz, CDCl_3) δ = 3.59–3.60 (m, 2H), 3.66–3.69 (m, 2H), 4.79 (br s, 1H), 7.69–7.74 (m, 2H), 8.23–8.26 (m, 2H), 9.97 (br s, 1H); ^{19}F NMR (376 MHz, CDCl_3 , ext. CF_3COOH) δ = –78.46 (d, J = 19.1 Hz, 1F), –69.83 (d, J = 19.1 Hz, 1F); EIMS m/z (%) 300 (M^+ ; 100), 299 (93), 285 (12), 105 (10). Anal. Calcd for $\text{C}_{16}\text{H}_{10}\text{F}_2\text{N}_2\text{O}_2$: C, 64.00; H, 3.36; N, 9.33%. Found: C, 63.84; H, 3.59; N, 8.98%.

3.3.5. 1,2-(1,4-Butanediamino)-3,4-difluoro-9,10-anthraquinone (**5e**)

Mp 231–232 °C; ^1H NMR (400 MHz, CDCl_3) δ = 1.81–1.84 (m, 2H), 1.90–1.93 (m, 2H), 3.46–3.50 (m, 2H), 3.76–3.81 (m, 2H), 4.15 (br s, 1H), 7.68–7.76 (m, 2H), 8.21–8.27 (m, 2H), 10.27 (br s, 1H); ^{19}F NMR (376 MHz, CDCl_3 , ext. CF_3COOH) δ = –69.76 (d, J = 21.7 Hz, 1F), –69.17 (d, J = 21.7 Hz, 1F); EIMS m/z (%) 328 (M^+ ; 31), 285 (100), 105 (13). Anal. Calcd for $\text{C}_{18}\text{H}_{14}\text{F}_2\text{N}_2\text{O}_2$: C, 65.85; H, 4.30; N, 8.53%. Found: C, 66.12; H, 4.39; N, 8.37%.

Table 4
Electrochemical measurement of anthraquinone dyes^a

Compound	E_{red} vs Ag	E_{ox} vs Ag
5c	–0.724	–0.483
5'c	–0.812	–0.743
14	–0.984	–0.698

^a All voltammograms were measured in an acetonitrile solution of tetrabutylammonium perchlorate (1 mmol dm $^{-3}$) at a scan rate of 100 mV s $^{-1}$ with a glassy-carbon working electrode, a platinum counter electrode, and a silver wire pseudo-reference electrode. The potential is referred to the internally added silver/silver nitrate (Ag/Ag $^+$) couple.

3.3.6. 6,7-Difluoro-9,12-dihydroxy-14H-naphtho[2,3-a]phenoxazine-8,13-dione (**6a**)

Mp > 300 °C; ¹H NMR (400 MHz, CDCl₃) δ = 6.68 (d, *J* = 7.3 Hz, 1H), 6.85–6.87 (m, 2H), 6.92–7.00 (m, 1H), 7.53 (dd, *J* = 5.8 and 3.3 Hz, 1H), 7.71 (dd, *J* = 5.8 and 3.3 Hz, 1H), 10.88 (s, 1H), 12.71 (s, 1H), 13.06 (s, 1H); ¹⁹F NMR (376 MHz, CDCl₃, ext. CF₃COOH) δ = –70.44 (d, *J* = 19.1 Hz, 1F), –60.83 (d, *J* = 19.1 Hz, 1F); EIMS *m/z* (%) 381 (M⁺; 100). Anal. Calcd for C₂₀H₉F₂NO₅: C, 63.00; H, 2.38; N, 3.67%. Found: C, 63.37; H, 2.51; N, 3.41%.

3.3.7. 6,7-Difluoro-9,12-dihydroxynaphtho[2,3-a]-oxanthrene-8,13-dione (**6b**)

Mp 254–255 °C; ¹H NMR (400 MHz, CDCl₃) δ = 7.00–7.16 (m, 4H), 7.31 (s, 2H), 12.84 (s, 1H), 13.00 (s, 1H); ¹⁹F NMR (376 MHz, CDCl₃, ext. CF₃COOH) δ = –67.57 (d, *J* = 19.7 Hz, 1F), –60.00 (d, *J* = 19.7 Hz, 1F); EIMS *m/z* (%) 382 (M⁺; 100), 191 (13). Anal. Calcd for C₂₀H₈F₂O₆: C, 62.84; H, 2.11%. Found: C, 63.11; H, 2.40%.

3.3.8. 6,13-Difluoro-8,11-dihydroxynaphtho[2,3-b]-oxanthrene-7,12-dione (**6b'**)

Mp > 300 °C; ¹H NMR (400 MHz, CDCl₃) δ = 7.06–7.08 (m, 4H), 7.31 (s, 2H), 12.84 (s, 2H); ¹⁹F NMR (376 MHz, CDCl₃, ext. CF₃COOH) δ = –57.47 (s, 2F); EIMS *m/z* (%) 382 (M⁺; 100), 354 (6), 325 (5). Anal. Calcd for C₂₀H₈F₂O₆: C, 62.84; H, 2.11%. Found: C, 62.61; H, 2.37%.

3.3.9. 6,7-Difluoro-9,12-dihydroxy-14H-naphtho[2,3-a]phenothiazine-8,13-dione (**6c**)

Mp > 300 °C; ¹H NMR (400 MHz, CDCl₃) δ = 6.70 (d, *J* = 7.4 Hz, 2H), 6.90–6.94 (m, 2H), 7.52–7.54 (m, 1H), 7.70–7.72 (m, 1H), 11.98 (s, 1H), 12.74 (s, 1H), 13.04 (s, 1H); ¹⁹F NMR (376 MHz, CDCl₃, ext. CF₃COOH) δ = –64.40 (d, *J* = 20.3 Hz, 1F), –45.25 (d, *J* = 20.3 Hz, 1F); EIMS *m/z* (%) 397 (M⁺; 100), 365 (15), 336 (10). Anal. Calcd for C₂₀H₉F₂NO₄S: C, 60.45; H, 2.28; N, 3.53%. Found: C, 60.30; H, 2.39; N, 3.94%.

3.3.10. 9,12-Dichloro-6,7-difluoro-14H-naphtho[2,3-a]phenothiazine-8,13-dione (**7c**)

Mp > 300 °C; ¹H NMR (400 MHz, CDCl₃) δ = 6.79 (d, *J* = 8.9 Hz, 1H), 6.88–6.90 (m, 2H), 7.03–7.08 (m, 1H), 7.62–7.67 (m, 2H), 11.31 (s, 1H); ¹⁹F NMR (376 MHz, CDCl₃, ext. CF₃COOH) δ = –69.00 (d, *J* = 21.4 Hz, 1F), –45.65 (d, *J* = 21.4 Hz, 1F); EIMS *m/z* (%) 437 (M⁺ + 4; 15), 435 (M⁺ + 2; 72), 433 (M⁺; 100), 398 (33), 397 (66). Anal. Calcd for C₂₀H₇Cl₂F₂NO₂S: C, 55.32; H, 1.62; N, 3.23%. Found: C, 55.17; H, 1.48; N, 3.47%.

3.3.11. 11H,18H-11,18-Diaza-5,6-dioxatrinaphthylene-12,17-dione (**8**)

Mp 250 °C (dec); ¹H NMR (400 MHz, CDCl₃) δ = 6.71 (d, *J* = 7.4 Hz, 2H), 6.85 (d, *J* = 7.4 Hz, 2H), 6.89–6.93 (m, 4H), 7.72–7.75 (m, 2H), 8.30–8.33 (m, 2H), 12.12 (s, 2H); EIMS *m/z* (%) 418 (M⁺; 100), 389 (9), 209 (14). Anal. Calcd for C₂₆H₁₄N₂O₄: C, 74.64; H, 3.37; N, 6.70%. Found: C, 74.57; H, 3.58; N, 6.58%.

3.3.12. 18H-18-Aza-5,6,11-trioxatrinaphthylene-12,17-dione (**9**)

Mp > 300 °C; ¹H NMR (400 MHz, CDCl₃) δ = 6.64 (dd, *J* = 7.7 and 1.5 Hz, 1H), 6.78–6.82 (m, 1H), 6.85–6.88 (m, 1H), 6.99–7.04 (m, 2H), 7.15 (dd, *J* = 7.1 and 2.3 Hz, 1H), 7.72–7.74 (m, 2H), 8.23 (dd, *J* = 5.7 and 3.2 Hz, 2H), 8.27 (dd, *J* = 5.7 and 3.2 Hz, 2H), 11.36 (s, 1H); EIMS *m/z* (%) 419 (M⁺; 100), 362 (9), 334 (7). Anal. Calcd for C₂₆H₁₃NO₅: C, 74.46; H, 3.12; N, 3.34%. Found: C, 74.32; H, 2.78; N, 3.54%.

3.3.13. 11H,18H-11,18-Diaza-5-oxa-6-thiatrinaphthylene-12,17-dione (**10**)

Mp 310 °C (dec); ¹H NMR (400 MHz, CDCl₃) δ = 6.65 (d, *J* = 6.7 Hz, 1H), 6.70–7.01 (m, 7H), 7.73–7.76 (m, 2H), 8.23–8.36 (m, 2H), 11.39 (s, 1H), 12.22 (s, 1H); EIMS *m/z* (%) 434 (M⁺; 100), 402 (29), 217 (18). Anal. Calcd for C₂₆H₁₄N₂O₃S: C, 71.88; H, 3.25; N, 6.45%. Found: C, 72.13; H, 3.18; N, 6.61%.

3.3.14. 6,7-(1,2-Ethanediamino)-9,12-dihydroxynaphtho[2,3-a]phenoxazine-8,13-dione (**11**)

Mp 252–254 °C; ¹H NMR (400 MHz, CDCl₃) δ = 3.55 (br, 2H), 3.68 (br, 2H), 4.74 (br, 1H), 6.71–6.77 (m, 2H), 6.84–6.88 (m, 2H), 7.67–7.70 (m, 2H), 8.28–8.34 (m, 2H), 10.90 (br, 1H), 12.07 (br, 1H); EIMS *m/z* (%) 369 (M⁺; 100), 353 (10), 184 (18). Anal. Calcd for C₂₂H₁₅N₃O₃: C, 71.54; H, 4.09, N, 11.38%. Found: C, 71.23; H, 3.84; N, 11.53%.

3.3.15. 5,6,11,18-Tetraoxatrinaphthylene-12,17-dione (**12**)

Mp > 300 °C; ¹H NMR (400 MHz, CDCl₃) δ = 7.01–7.07 (m, 6H), 7.14–7.16 (m, 2H), 7.76 (dd, *J* = 5.7 and 3.3 Hz, 2H), 8.22 (dd, *J* = 5.7 and 3.3 Hz, 2H); EIMS *m/z* (%) 420 (M⁺; 100), 279 (7), 260 (6), 250 (7). Anal. Calcd for C₂₆H₁₂O₆: C, 74.29; H, 2.88%. Found: C, 74.31; H, 3.04%.

3.3.16. 11H-11-Aza-5,18-dioxa-6-thiatrinaphthylene-12,17-dione (**13**)

Mp > 300 °C; ¹H NMR (400 MHz, CDCl₃) δ = 6.70 (d, *J* = 7.7 Hz, 1H), 6.81–6.90 (m, 2H), 6.98–7.04 (m, 4H), 7.14 (d, *J* = 7.7 Hz, 1H), 7.75 (dd, *J* = 5.8 and 2.5 Hz, 2H), 8.25 (dd, *J* = 5.8 and 2.5 Hz, 2H), 12.53 (s, 1H); EIMS *m/z* (%) 435 (M⁺; 100), 406 (7), 350 (10),

217 (13). Anal. Calcd for $C_{26}H_{13}NO_4S$: C, 71.71; H, 3.01; N, 3.22%. Found: C, 72.05; H, 3.01; N, 3.27%.

3.3.17. 11H,18H-11,18-Diaza-5,6-dithiatrinaphthylene-12,17-dione (**14**)

Mp 236 °C (dec); (lit. [17] 246–247 °C).

3.3.18. 11H,18H-13,16-Dichloro-11,18-diaza-5,6-dithiatrinaphthylene-12,17-dione (**15**)

Mp > 300 °C; 1H NMR (400 MHz, $CDCl_3$) δ = 6.80 (d, J = 7.6 Hz, 2H), 6.87 (t, J = 7.6 Hz, 2H), 7.05 (d, J = 7.6 Hz, 2H), 7.14 (t, J = 7.6 Hz, 2H), 7.51 (br, 2H), 11.46 (s, 2H); EIMS m/z (%) 522 (M^+ + 4; 19), 520 (M^+ + 2; 80), 518 (M^+ ; 100), 486 (31). Anal. Calcd for $C_{26}H_{12}Cl_2N_2O_2S_2$: C, 60.12; H, 2.33; N, 5.39%. Found: C, 60.41; H, 2.00; N, 5.51%.

3.4. Synthesis of 11H,18H-13,16-bis[4-(methoxyphenyl)amino]-11,18-diaza-5,6-dithiatrinaphthylene-12,17-dione (**17**)

To *p*-anisidine (460 mg, 3 mmol) were added 11H,18H-13,16-dichloro-11,18-diaza-5,6-dithiatrinaphthylene-12,17-dione **15** (52 mg, 0.1 mmol) and sodium acetate (84 mg, 0.8 mmol) and the mixture was heated at 150 °C for 24 h. After the reaction was completed, the mixture was poured into brine (50 mL). The resulting precipitate was filtered, purified by column chromatography (SiO_2 , ethyl acetate/hexane = 1/3), and recrystallized from toluene. The physical and spectral data are shown below. Mp > 300 °C; 1H NMR (400 MHz, $CDCl_3$) δ = 3.83 (s, 6H), 6.67 (d, J = 7.3 Hz, 2H), 6.77 (t, J = 7.3 Hz, 2H), 6.90 (d, J = 8.5 Hz, 2H), 6.91 (d, J = 8.5 Hz, 2H), 6.97 (t, J = 7.3 Hz, 2H), 7.18 (d, J = 8.5 Hz, 4H), 7.23 (d, J = 7.3 Hz, 2H), 7.54 (br s, 1H), 7.70 (br s, 1H), 11.71 (s, 2H), 13.00 (s, 2H); EIMS m/z (%) 692 (M^+ ; 74), 347 (49), 346 (100), 339 (20). Anal. Calcd for $C_{40}H_{28}N_4O_4S_2$: C, 69.35; H, 4.07; N, 8.09%. Found: C, 69.18; H, 4.05; N, 7.88%.

4. Conclusions

The reaction of 1,2,3,4-tetrafluoro-9,10-anthraquinones with bifunctional nucleophiles afforded not only 1,2-cyclized but also symmetrically and unsymmetrically dicyclized derivatives. These products showed their λ_{max} in the range of 353–712 nm in dichloromethane. The melting point of fluorine-containing derivatives was not always lower than the fluorine-free derivatives. The introduction of electron-withdrawing fluorine atoms into anthraquinone derivatives did not improve the photostability.

References

- [1] Gregory P. High-technology applications of organic colorants. New York: Plenum Press; 1991.
- [2] Matsui M. Fluorine-containing dyes. J Jpn Soc Colour Mater 2000;73:553.
- [3] Krapcho AP, Avery Jr KL. Formation of N–N and N–C bond-cleavage products in displacements with *N,N*-disubstituted hydrazines on 1-halo- or 1,4-dihaloanthracene-9,10-diones. J Org Chem 1988;53:5927.
- [4] Morrow GW, Swenton JS, Filippi JA, Wolgemuth RL. Synthesis of 1-fluoro-4-fluoro- and 1,4-difluoro-4-demethoxydaunomycinone interesting D-ring analogues of adriamycin. J Org Chem 1987;52:713.
- [5] Krapcho AP, Getahun Z. Convenient synthetic route to 1,4-difluoroanthracene-9,10-dione. Synth Commun 1985;15:907.
- [6] Krapcho AP, Getahun Z, Avery Jr KL, Vargas KJ, Hacker MP. Synthesis and antitumor evaluations of symmetrically and unsymmetrically substituted 1,4-bis[(aminoalkyl)amino]anthracene-9,10-diones and 1,4-bis[(aminoalkyl)amino]-5,8-dihydroxyanthracene-9,10-diones. J Med Chem 1991;34:2373.
- [7] Loskutov VA, Nekrasova LN, Fokin EP. Reaction of polyhaloanthraquinones with nucleophilic reagents VII. Reaction of 1,2,3,4-tetrafluoroanthraquinone with diethyl-, dibutyl-, diisobutyl- and dibenzylamines. Izv Sib Otd Akad Nauk SSSR, Ser Khim Nauk 1970;119.
- [8] Fokin EP, Loskutov VA. Interaction of polyhaloanthraquinones with nucleophilic reagents. III. Effect of the association of amides by hydrogen bonding on the orientation of entering amino groups in 1,2,3,4-tetrafluoroanthraquinone. Zh Obshch Khim 1968;38:1884.
- [9] Fokin EP, Loskutov VA, Konstantinova AV. Reaction of polyhaloanthraquinones with nucleophilic reagents. I. Reaction of 1,2,3,4-tetrafluoroanthraquinone with ammonia methylamine and dimethylamine. Zh Obshch Khim 1967;37:391.
- [10] Fokin EP, Loskutov VA, Vol'skii LN. Reaction of polyhaloanthraquinones with nucleophilic reagents. III. Reaction of 1,2,3,4-tetrafluoroanthraquinone with sodium methoxide. Zh Obshch Khim 1970;6:1277.
- [11] Coe PL, Croll BT, Patrick CR. Aromatic polyfluoro-compounds XXXV 1,2,3,4-tetrafluoroanthraquinone and some reactions of tetrafluorophthalic acid derivatives. Tetrahedron 1967;23:505.
- [12] Gornostaev LM, Lavrikova TI, Arnol'd EV. Reaction of 1,2,3,4-tetrafluoro-9,10-anthraquinone with thiophenols. Zh Obshch Khim 1992;28:2291.
- [13] Masuda K, Aoki M, Kaieda O. Photosensitive resin composition for color filter preparation. Eur Pat Appl 833203; Chem Abstr 1998;128:288336 and patents cited therein.
- [14] Matsuoka M, Kim S-H, Kitao T. Novel synthesis of quinone-type I.R. dyes for optical recording media. Chem Commun 1985;1195.
- [15] Kim S-H, Matsuoka M, Kitao T. Novel synthesis of phenosele-nazinequinone infrared dyes. Chem Lett 1985;1351.
- [16] Kim S-H, Matsuoka M, Yodoshi T, Kitao T. Synthesis of functional anthraquinone dyes from tetrafluorophthalic anhydride. Chem Express 1986;1:129.
- [17] Kim S-H, Matsuoka M, Yodoshi T, Kitao T. Novel synthesis of anthraquinonoid near-infrared absorbing dyes. Dyes Pigments 1986;7:93.
- [18] Frisch MJ, Trucks GW, Schlegel HB, Scuseria GE, Robb MA, Cheeseman JR, et al. Gaussian 03W program. Pittsburgh, PA: Gaussian Inc.; 2003.
- [19] Uchiyama S, Santa T, Imai K. Fluorescence characteristics of six 4,7-disubstituted benzofuran compounds: an experimental and semi-empirical MO study. J Chem Soc Perkin Trans 2 1999;2525.
- [20] Peters AT, Tenny BA. Dyes for synthetic-polymer fibres 14H-naphtho[2,3-*a*]phenothiazine-8,13-diones and 1H-2,3-dihydroanthra[2,1-*b*][1,4]thiazine-7,12-diones. Dyes Pigments 1980;1:91.

- [21] Loskutov VA, Nekrasova LN, Konstantinova AV. Fluorine-19 nuclear magnetic resonance spectra of 1-(alkylamino)-2,3,4-trifluoro- and 2-(alkylamino)-1,3,4-trifluoroanthraquinones. *Izv Sib Otd Akad Nauk SSSR, Ser Khim Nauk* 1970; 5:108.
- [22] Kölliker HP, Caveng P. Kondensationen mit aliphatic und zykoaliphatischen amines imines und diaminen in der anthrachinonreihe. *Chimia* 1966;20:281.
- [23] Tanaka Y, Ohki Y, Ishii Y. Photodecomposition of amino anthraquinone disperse dyes in organic solvents. *Sen'I Gakkai Shi* 1968;24:132. *Chem Abstr* 1968;69:44549q.
- [24] Mckellar JF. Phototendering of the anthraquinone vat dyes a review. *Radiat Res Rev* 1971;3:141. and references cited therein.
- [25] Shimamura T, Nishihara M, Masumi N. Synthesis of 1-alkylaminoanthraquines derivatives. JP H08-259508. *Chem Abstr* 1997;126:33022.